

Accepted Manuscript

Fabrication of porous disk-like Ni/NiO microwave absorber and its excellent broad frequency absorption performance

Yuhang Guo, Songtao Dong, Suwei Liu, Ye Cheng, Zhenya Zhang, Hongying Wang



PII: S0925-8388(17)33276-0

DOI: [10.1016/j.jallcom.2017.09.226](https://doi.org/10.1016/j.jallcom.2017.09.226)

Reference: JALCOM 43282

To appear in: *Journal of Alloys and Compounds*

Received Date: 22 February 2017

Revised Date: 18 September 2017

Accepted Date: 21 September 2017

Please cite this article as: Y. Guo, S. Dong, S. Liu, Y. Cheng, Z. Zhang, H. Wang, Fabrication of porous disk-like Ni/NiO microwave absorber and its excellent broad frequency absorption performance, *Journal of Alloys and Compounds* (2017), doi: 10.1016/j.jallcom.2017.09.226.

This is a PDF file of an unedited manuscript that has been accepted for publication. As a service to our customers we are providing this early version of the manuscript. The manuscript will undergo copyediting, typesetting, and review of the resulting proof before it is published in its final form. Please note that during the production process errors may be discovered which could affect the content, and all legal disclaimers that apply to the journal pertain.

Fabrication of Porous Disk-like Ni/NiO Microwave Absorber and Its Excellent Broad Frequency Absorption Performance

Yuhang Guo ^{a,*}, Songtao Dong ^a, Suwei Liu ^b, Ye Cheng ^a, Zhenya Zhang ^c, Hongying Wang ^{d,**}

^a*School of Materials Science and Engineering, Jiangsu University of Science and Technology, Zhenjiang, Jiangsu, 212003, China*

^b*Engineering Training Center, Nantong University, Nantong, Jiangsu, 226019, China*

^c*School of Material Science and Engineering, Jiangsu University, Zhenjiang, 212013, China*

^d*School of Materials Science and Engineering, Jiamusi University, Jiamusi, Heilongjiang, 154007, China*

* Corresponding Author :

Prof Dr. Yuhang Guo

Tel./fax: +86 511 84401188

. E-mail addresses: guoyuhang@just.edu.cn

**Corresponding Author:

Prof Dr. Hongying Wang

Tel./fax: +86 454 8618701.

E-mail addresses: wanghongying_hm@163.com

Abstract:

This research reports a novel porous disk-like Ni/NiO binary composite with the diameter of disk ranged in 100-200 nm and the size of the porous distributed in 5-10 nm. The absence of Ni was generated by the partial reduction of NiO. This porous Ni/NiO product owns the matched impedance matching and attenuation electromagnetic wave ability since the moderate complexed permittivity and improved permeability value. In this regard, this composite proves to be desired electromagnetic absorber to treat the increasingly electromagnetic interference issue (EMI). The qualified absorption frequency bandwidth of the optimal Ni/NiO product covers 6.4 GHz (11.2-17.6 GHz) under the coating layer thickness of 1.5 mm. The excellent electromagnetic absorption properties have been discussed in depth. The unique porous structure benefits to the electromagnetic absorption performance which is due to the suppressed eddy current effect.

Key words: porous disk-like, Ni/NiO, electromagnetic interference, qualified absorption frequency, eddy current effect.

1: Introduction:

Because of the exposure application of wireless communication, local area networks, radar detector devices, the problem of electromagnetic interference (EMI) has possess a negative role on our daily life. [1-2] Therefore, an available method to settle such a problem is to explore a high-performance electromagnetic absorber to eliminate this electromagnetic interference issue. [3] As we know, before to attenuate the electromagnetic wave, the electromagnetic absorption layer can let the indent electromagnetic wave enter in and decrease the interface reflection. In this regard, a good impedance matching performance is expected to achieve for the absorber. [4-5] Based on the electromagnetic absorption mechanism, decrease the complex permittivity parameter or improve the permeability value are the efficient strategy to reach a good impedance matching behavior. [6] Based on the above consideration, a few ferrites thus have attracted intense interests. The complex permittivity value of ferrites is ranged in the moderate region. Meanwhile, the magnetic properties of ferrite will reach an improvement complex permeability value as compared to nonmagnetic absorber. [7-8] However, ferrites are suffered from the poor attenuation ability and limited their applications, especially the dielectric loss ability. [9-11] It is widely believed that the dielectric loss behavior is resulting from the polarization and conductive loss. The high-frequency (>GHz) polarization form is primary resulting from the interface polarization. [12-13]. Owing to

the weakly conductive loss and polarization ability, thus ferrites are hard to present the good performance on the electromagnetic absorption properties. Based on above consideration, design of metal/metal oxide binary composites has been proved to be an efficient strategy to strong the polarization intensity with the below advantages. [14]. On the one hand, the absence of metal in metal/metal oxide benefits to the conductive loss intensity since the improved conductive value. On the other hand, the interface between metal and metal oxide is enable to boost the polarization intensity. As a result, the dielectric loss can be boosted." [15] Zn/ZnO product was prepared by the reduction strategy and the RL_{\min} value was -23.0 dB. [16] Zhao *et.al.* used the hydrothermal method to prepare Ni/SnO₂ absorber and the minimum reflection loss value was up to be -37.6 dB. [17] Recent findings revealed that these types of metal/metal oxides are suffered from the eddy current. [18] According to the electromagnetic absorption theory, the eddy current effect happens at magnetic absorber and prevents the electromagnetic wave enter into the absorption layer which should be suppressed. [19] Design of porous metal/metal oxide composite is able to suppress this unwanted eddy current effect, according to Ji's review. [20] For example, the porous 3-dimentional flower-like Co/CoO composite was synthesized by Lv *et.al* and the optimal reflection loss value was up to -50.0 dB. [21] The electromagnetic absorption properties of porous cube-like Fe/SiO₂ also have been researched by Yang *et.al* and the optimal absorption value was approximately -50 dB. [22]

In this research, the electromagnetic absorption properties of porous disk-like Ni/NiO was investigated. NiO was obtained at the initial stage and subsequently followed reduction process, the Ni was generated and resulted in the Ni/NiO binary composite. This product presented the novel electromagnetic absorption properties.

2: Experimental Section:

2.1 Fabrication of porous disk-like NiO sample.

Porous disk-like NiO was synthesized by a simple hydrothermal method. In a typical process, 500 mg anhydrous nickel chloride (NiCl₂) was dissolved in 50 ml of distilled water with ultrasonic treatment for 30 min. Then, ammonia solution was dropwise into the solution and the control the PH value to 10. Afterward, the transparent solution was added into the autoclave (100 mL) for hydrothermal reaction at 160 °C for 10 h. The obtained precipitate was collected and then washed 3-5 times. Finally, the precipitate was dried at 80 °C for 24 h. Porous disk-like NiO (denote as S1)

was obtained by annealed in a tube furnace at 400 °C for 5 h in air.

2.2 Preparation of Ni/NiO composite:

"The Ni/NiO composite was prepared by another hydrothermal method. Typically, 100 mg of disk-like NiO and a certain volume of ammonia were dissolved in 30 mL distilled water and stirring 30 min. The PH value should be ranged in the region of 12~14. Then, hydrazine hydrate was added into the above solution as the reduce agent to transfer the NiO into metal. After 5 mins, the mixture solution was transferred into a 100 mL autoclave and heated at 150 °C for 20 h. The samples obtained with 5, 10,15 mL of hydrazine hydrate were denoted as S2 S3 and S4, respectively."

2.3 Characterization

The power X-ray diffraction (XRD) patterns spectral were obtained by a Bruker D8 X-ray diffraction using Cu K α radiation ($\lambda=0.154178$ nm). The magnetic properties of coercive force and magnetization were examined by a vibrating sample magnetometer (VSM, Lakeshore, Model 7400 series) at 298 K. The XPS spectrum was obtained with a PHI 5000 VersaProbe systems which an Al K α X-ray source operating at 150 W. The magnetization hysteresis curves of the samples were conducted by a vibration sample magnetization (VSM, Lakeshore, Model 7400 series). The electromagnetic parameters of these products were measured using the coaxial-line method utilizing an Agilent Network Analyzer N5230 and the tested frequency was in the range of 2-18 GHz. The sample was prepared by homogenously mixing the paraffin wax with 50 wt% of the sample and then compressing into toroidal-shaped samples with 7.0 mm in outer diameter and 3.04 mm in inner diameter. In this way, the electromagnetic parameters (includes ϵ' , ϵ'' , μ' , μ'') could be obtained. The reflection loss curves could be drawn by inputting the electromagnetic parameters into the below formulas (1) and (2): [23-26]

$$Z_{in}=Z_0(\mu_r/\epsilon_r)^{1/2}\tanh[j(2\pi fd(\mu_r\epsilon_r)^{1/2}/c)] \quad (1)$$

$$RL(\text{dB})=20\log|(Z_{in}-Z_0)/(Z_{in}+Z_0)| \quad (2)$$

Where Z_{in} is the input impedance of the absorber, f is the frequency of electromagnetic wave, d is the coating thickness of the absorber while c is the velocity of electromagnetic wave in free space. ϵ_r ($\epsilon_r=\epsilon'-j\epsilon''$) and μ_r ($\mu_r=\mu'-j\mu''$) are the complex permittivity and permeability of the absorber.

3: Results and Discussion:

Figure 1a shows the XRD patterns of the as prepared composite under addition of 10 mL

hydrazine hydrate. The diffraction peaks at 37.2, 43.2, and 62.8° can be assigned, respectively to (101), (012) (110) crystal planes of the NiO (JSPDF card no: 44-1159). Whereas, the sharply diffraction peaks at 44.5, and 51.8 ° can be indexed to the (111) and (200) crystal planes of metal Ni (JSPDF card no: 04-0850). There are no any other impurities peaks could be observed. In Figure 1b, the porous disk-like shaped structure could be observed in the TEM images. The size of each disk ranges in 80-100 nm. Magnify the image, the diameters of these porous are distributed in the range of 5-10 nm, as seen in the Figure 1c. The HR-TEM images reveals that there are two types of lattice fringes, with the lattice spacing d values of 0.241 and 0.202 nm, which are ascribed to the (111) plane of NiO and (111) plane of metal Ni, respectively.

The atomic ratios of Ni/NiO are easily controlled by tuning the volume of hydrazine hydrate. Without addition of the reduction agent, the obtained product is NiO (denoted as S1), as seen in the Figure 2a. If more the hydrazine hydrate ($V=20$ mL) was added, the initial porous NiO was totally converted into metal Ni (S4), as proved by the XRD patterns (Figure 2a). If the volume of reduction agent is fixed at 5 and 10 mL, the phase compositions of obtained samples are Ni and NiO. The TEM images of S1, S2 and S4 were showed in Figure S1(Support information). Actually, all of these products show disk-like structure. The size of porous is larger with more volumes of hydrazine hydrate.

In this research, the Ni/NiO products reduced by 5 and 10 mL are denoted as S2 and S3, respectively. To analyze the atomic ratios of Ni/NiO, X-ray photoelectron (XPS) technique as an efficient way to analysis the composite and valance state, as presented in Figure 2 b-c. [27-30]

By fitting the Ni 3/2p peak, the metal Ni and NiO characterized peaks can be obtained with the binding energy value of 852.0, 854.2 eV, respectively. [31] The surface area ratios of Ni and NiO peaks are estimated to be 1:4 and 2:1 for S2 and S3, suggesting their atomic ratios. It is widely believed that the larger magnetization value will lead to the bigger magnetic loss and improvement impedance matching behavior, since the enhancement of complex permeability value. [32] The magnetization values were obtained on a vibrating sample magnetometer. In Figure 3, the magnetization values are 0, 14.2, 32.8, 48.2 emu/g for the S1, S2, S3 and S4 products

3.2: The Electromagnetic Absorption Properties:

The electromagnetic absorption properties of these products are shown in Figure 4. To evaluate the electromagnetic absorption property of one absorber, the qualified frequency bandwidth (also

called as effective absorption frequency region) referring to the region of RL_{min} value less than -10 dB should be as broader as possible. At the same time, a good electromagnetic absorption property should be obtained within a small absorption layer thickness (d). [33] To see the Figure 4a, all the RL_{min} values calculated at 1.5-3.0 mm are smaller than -5.0 dB for S1, indicating the poor electromagnetic absorption properties. As for S2 product, the effective absorption bandwidth at 1.5 mm reached 2.2 GHz (15.8~18 GHz). When the absorption layer thickness more than 2.0 mm, the absorption frequency bandwidth is smaller than 2.0 GHz. The qualified absorption frequency bandwidth at 1.5 mm improves to 6.4 GHz (11.2~17.6 GHz) for S3. Even so, the qualified absorption bandwidth of S3 still are larger than 4.0 GHz at 2.0 and 2.5 mm. While for S4, the minimum reflection loss values are all bigger than -10 dB and thus have no qualified absorption region.

To better understanding the difference in the electromagnetic absorption properties, the electromagnetic parameters have been given in the Figure 5-6. It is widely believed that the electromagnetic parameters influence both the impedance matching and attenuation (including dielectric and magnetic loss ability) ability. By this way, the final electromagnetic absorption properties can be achieved and thus indirectly decides the final electromagnetic absorption properties. [34] Figure 5 lists the permittivity parameters (ϵ'/ϵ'') of S1-S4 products. The electromagnetic absorption theory reveals that the real part permittivity value (ϵ') refers to the storage electrical ability while the imaginary part of permittivity value (ϵ'') means the dielectric loss ability which composed by the polarization and conductive loss behavior (ϵ''). [35] In Figure 5a, the ϵ' value of S1 is ~3.2 at whole frequency region and the ϵ'' value is almost approximately 0. In Figure 5b, due to the presence of Ni, the value of S2 improves to 8.4-8.0. Meanwhile, the ϵ'' value improved to 1.9-3.3 which probably attributes to the stronger conductive loss ability. At higher frequency region (12-18 GHz), two obvious peaks can be seen. These two peaks may relate to the interface polarization effect at the Ni and NiO interface. [36-37] As for S3, the ϵ'' value also further increases to 12.2-12.0. Similar two peaks also can be found at S3 (seen Figure 5c). After the NiO totally be reduced to Ni, both the ϵ' and ϵ'' values present the sharply increase, representing the strongest conductive ability. Besides, the two peaks disappeared which probably due to disappeared Ni and NiO interface, as shown in Figure 5d.

The permeability parameters have been given in Figure 6. Similarly, the real part of permeability

(μ') value means the storage magnetic ability and the imaginary part of permeability refers to the magnetic loss ability. [38] For nonmagnetic material, the μ' value is ~ 1.0 and the μ'' value is almost 0, like carbon materials. [39-41] As seen the Figure 6b, the μ' value of S2 is larger than 1.0 (1.23-1.15). For S3, the μ' value is further increases to 1.31-1.18 and μ'' value in the region of 0.5-0.1 (seen Figure 6c). In Figure 6d, the μ' value of S4 is 1.4-1.2 and μ'' value is nearly 0.25. One conclusion can be made that the improvement of Ni atomic ratio will lead to the stronger magnetic loss ability.

Generally, the attenuation constant α represents the integral attenuation ability including magnetic and dielectric loss ability which can be expressed by the below equation: [42]

$$\alpha = \frac{\sqrt{2\pi f}}{c} \times \sqrt{(\mu\epsilon' - \mu\epsilon'') + \sqrt{(\mu\epsilon' - \mu\epsilon'')^2 + (\mu\epsilon'' + \mu\epsilon')^2}} \quad (3)$$

It could be observed from Figure 7 that S4 presents the largest attenuation value among these samples which is due to the contribution of conductive and magnetic loss ability. S1 owns the lowest attenuation constant value α value. This is primary reason why S1 shows the poorest electromagnetic absorption properties. However, S4 was suffered from the poor impedance matching ability which is due to the larger ϵ_r value ($\epsilon_r = \epsilon' - j\epsilon''$). S3 with the optimal absorption properties can be attributed to the matched impedance matching and attenuation ability.

The porous structure also benefits to the electromagnetic absorption properties since the suppressed eddy current. As we know, eddy current effect generally happens at the magnetic material. [43] Although eddy current loss is one of the magnetic form, the generated circle current will prevent the incident electromagnetic wave enter into the absorption. For example, the microwave absorption properties of flaky carbonyl iron were no more than -10 dB. [44] The optimal reflection loss value of spherical-shape Ni is also bigger than -10 dB. [45] The poor electromagnetic absorption properties of these magnetic materials all attributed to the current eddy effect. Design porous structure has been considered to be an efficient route to prevent the fabrication of circle eddy, according to current literature. [46] To best of our knowledge, the eddy current effect could be expressed in the below equation: [47]

$$C_o = \mu''(\mu')^{-2} f^1 = 2\pi\mu_0 d^2 \delta$$

Where δ is the electric conductive. If the eddy current effect happens at the magnetic material the C_o will be a constant at tested frequency. If not, it means the current effected did not

happened on this material. As seen in Figure 8 a-d, the C_o values of the four samples are changeable at 2-18 GHz.

4: Conclusion:

The Ni/NiO binary composite with porous disk-like structure has been introduced in this research. Firstly, porous disk-like NiO was prepared by a simple hydrothermal process and followed by another hydrothermal reduction route, partial NiO can be converted into metal Ni and resulted in magnetic Ni/NiO porous disk-like structure. This binary composite presented the moderate impedance matching and attenuation ability if applied as electromagnetic absorber to treat the electromagnetic interference issue. The calculated electromagnetic absorption results revealed that the qualified absorption frequency of this optimal Ni/NiO composite was up to 6.4 GHz (11.2-17.6 GHz) which was much better than single component of NiO or Ni. The excellent electromagnetic properties were proposed in this research which were attributed to the probable conductive loss. At the same time, the interface between Ni and NiO also benefited to the attenuation of electromagnetic wave.

References:

- [1] H. J. Wu, G. L. Wu, Y. Y. Ren, L. Yang, L. D. Wang, X. H. Li, *J. Mater. Chem. C*, 3(2015):7677-7690.
- [2] J. S. Deng, S. M. Li, Y. Y. Zhou, L. Y. Liang, B. Zhao. *J. Colloid. Interf. Sci.* 509 (2018):406-413.
- [3] H. L. Lv; Y. H. Guo; Y. Zhao; H. Q. Zhang; B. S. Zhang; G. B. Ji; Z. C. J. Xu. *Carbon*. 110(2016): 130-137.
- [4] J. S. Deng, Q. B. Wang, Y. Y. Zhou, R. Zhang, *RSC Adv.* 7(2017):9294-9302.
- [5] Y. H. Guo; S. W. Liu; Z. Y. Zhang; S. T. Dong; H. Y. Wang; *J. Alloys. Compd.* 684(2016): 549-555.
- [6] H. L. Lv, G. B. Ji, X. H. Liang, H. Q. Zhang, Y. W. Du. *J. Mater. Chem. C* 3(2015):5056-5064.
- [7] X. G. Huang.; J. Zhang.; W. F. Rao.; T. Y. Sang.; B. Song.; C. P. Wang.; *J. Alloy. Compd.* 662(2016): 409-414.
- [8] J. Zhao.; J. Yu.; Y. Xie.; Z. G. Le.; X. W. Hong.; S. Q. Ci.; J. H. Chen.; X. Y. Qing.; W. J. Xie.;

- Z. H. Wen. *Sci. Repts.* 6(2016): 20496-20507.
- [9] R.L. Ji.; C.B. Cao.; Z. Chen.; H.Z. Zhai.; J. Bai.; *J. Mater. Chem. C* 2(2014): 5944-5953
- [10] Z. H. Yang.; Z. W. Li.; Y.H. Yang.; Z. C. J. Xu.; *ACS Appl. Mater. Interfaces* 6(2014): 21911-21915
- [11] M. Fu.; Q.Z. Jiao.; Y. Zhao.; *J. Mater. Chem. A* 1(2013): 5577-5586
- [12] Y.F. Pan.; G. S. Wang.; L. Liu.; L. Guo.; S. H. Yu. *Nano Res.* 10(2017) :284-294.
- [13] H.L. Lv, X.H. Liang, Y. Cheng, H.Q. Zhang, D.M. Tang, B.S. Zhang, G.B. Ji, *ACS Appl. Mater. Interfaces.* 7(2015):4744-4750.
- [14] Y.P. Duan; Z. Liu; H. Jing; Y. H. Zhang and S. Q. Li. *J. Mater. Chem.* 22(2012)18291-18299.
- [15] Y. Liu, Y. N. Li.; K. Jiang.; G.X. Tong.; T. X. Lv.; W. H. Wu. *J. Mater. Chem. C.* 4(2016) :7316-7323.
- [16] B. Zhong, X. H. Tang, X.X. Huang, L. Xia, X.D. Zhang, G.W. Wen, Z. Chen, *CrystEngComm.* 17(2015): 2806-2814.
- [17] B. Zhao, W. Y. Zhao, G. Shao, B. B. Fan, R. Zhang, *Dalton Trans.* 44(2015):15984-15993.
- [18] X. G. Liu.; D. Y. Geng.; H. Meng.; P. J. Shang.; Z. D. Zhang.; *Appl. Phys. Lett.* 92(2008):173117-173120.
- [19] S. S. Kim.; S.T. Kim.; Y.C. Yoon.; K. S. Lee.; *J. Appl. Phys.* 97(2005)2117-2122.
- [20] H. L. Lv, Y. H. Guo, Z. H. Yang, Y. Cheng, L. Y. P. Wang, B. S. Zhang, Y. Zhao, Z. C. J. Xu. *J. Mater. Chem. C* 5(2017):491-512.
- [21] H.L. Lv; X.H. Liang; G.B. Ji; H.Q. Zhang; Y.W. Du. *ACS Appl. Mater. Interfaces.* 7(2015), 9776-9783.
- [22] Z. H. Yang.; Z. W. Li.; L. H. Yu.; Y. H. Yang.; Z. C. J. Xu. *J. Mater. Chem. C.* 2(2014) 7583-7588.
- [23] Y. C. Yin, M. Zeng, J. Liu, W. K. Tang, H. R. Dong, R.Z. Xia, R. H. Yu, *Sci. Rep.* 6(2016)25075-25084.
- [24] S. W. Liu, Y. H. Guo, S.T. Dong, Y. Cheng, Z. Y. Zhang, H. Y. Wang, *J. Alloy. Compld.* 711(2017):184-189.
- [25] H. J. Wu, G. L. Wu, L. D. Wang, *Powder Technol.* 269(2015):443-451.

- [26] H. L. Lv, G. B. Ji, W. Liu, H. Q. Zhang, Y. W. Du. *J. Mater. Chem. C* 3(2015):10232-10241.
- [27] J. S. Deng, Y. H. Lei, S. M. Wen, Z. X. Chen, *Int. J. Miner Process.* 140(2015)43-49.
- [28] G. L. Wu, H. J. Wu, K. K. Wang, C. H. Zheng, Y. Q. Wang, A. L. Feng, *RSC Adv.* 6(2016):58069-58076.
- [29] H. J. Wu, G. L. Wu, Q. F. Wu, L. D. Wang, *Mater. Charact.* 97(2014): 18-26.
- [30] J. S. Deng, Y. B. Mao, S. M. Wen, Y. J. Xian, J. Liu, *Int. J. Min. Met. Mater.* 22(2015):111-116.
- [31] Y. S. Chen.; J. F. Kang.; B. N. Chen.; E. G. Wang.; *J. Phys. D: Appl. Phys.* 45(2012):065303-065309.
- [32] X. L. Zhang.; J. Feng.; Y. Zong.; H. Miao.; X. Y. Hu.; J. T. Bai.; X. H. Li. *J.Mater.Chem.C.3(2015):4452-4463.*
- [33] H. L. Lv, Y. H. Guo, G. L. Wu, G. B. Ji, Y. Zhao, Z. C. J. Xu. *ACS Appl. Mater. Interfaces.* 9(2017):5660-5668.
- [34] G. P. Wan.; G. Z. Wang.; X. Q. Wang.; H. N. Zhao.; X. Y. Li.; K. Wang.; L. Yu.; X. G. Peng.; Y. Qin. *Dalton Trans.* 44(2015): 18804-18809.
- [35] H. J. Wu.; G. L. Wu.; L. D. Wang. *Power. Technol.* 269(2015):443-451.
- [36] H.L. Lv.; H. Q. Zhang.; G. B. Ji.; Z. C.J. Xu.; *ACS Appl. Mater. Interfaces.* 8(2016):6529-6538.
- [37] Y. Akinay, F.Hayay, Y.Kanbur, H. Gokkaya, S.Polat. *Polym Composite.* DOI: 10.1002/pc.24487.
- [38] A. Shah.; A. Ding.; Y.H. Wang.; L. Zhang.; D. X. Wang.; J. Muhammad.; H. Huang.; Y. P. Duan.; X. L. Dong.; Z. Z. Zhang.; *Carbon*, 95(2016)987-997.
- [39] J. S. Deng, S. M. Wen, Y. J. Xian, J. Liu, S. J. Bai, T. Nanferr. *Metal Soc.*24(2014):3955-3963.
- [40] J. H. Zhang, J. Du, H. L. Wang, J. L. Wang, Z. K.Qu, L. Jia. *Mater. Letter.* 65(2011)2565-2567.
- [41] J.H.Zhang, B.Yang, F.Zhang, *CrystEngComm.* 14(2012):3451-3455.
- [42] H. L. Lv, H. Q. Zhang, J. Zhao, G. B. Ji, Y. W. Du. *Nano Res.* 9(2016):1813-1822.
- [42] M. Zong.; Y. Huang.; N. Zhang. *Appl. Mater. Sci.* 345(2015) 272-278.

[44] X. H. Ren.; H. Q. Fan.; Y. K. Cheng.; Appl. Phys. A. 122(2016) 506-512.

[45] B. Zhao.; G. Shao.; B. B. Fan.; W. Y. Zhao.; R. Zhang.; RSC Adv. 4 (2014) 57424-57429.

[46] C.Z.Hu.; S. Qiu.; X.Z. Wang.; J. R. Liu.; L. Q. Luan.; W. Liu.; M. Ttoh.; K. Machid.; J. Mater. Chem. 22(2012)22160-22166.

[47] J. Guo, X. Wang, P. Miao, X. Liao, W. Zhang and B. Shi. J. Mater. Chem. 22(2012): 11933-11942.

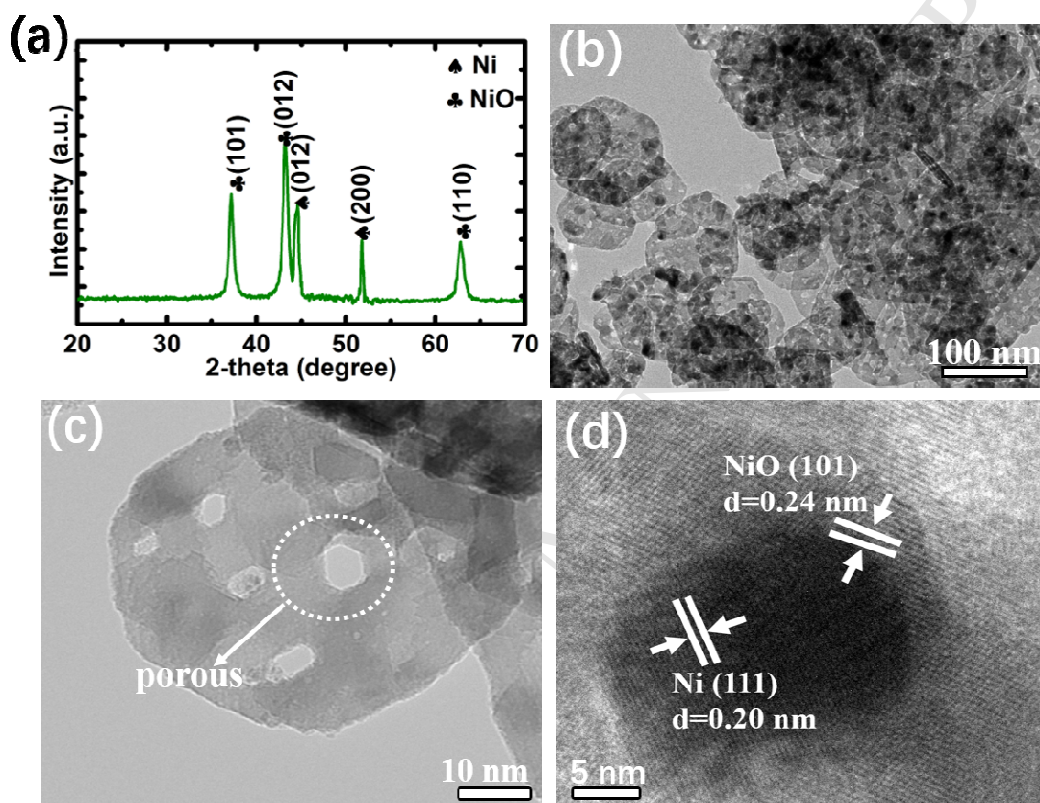


Figure 1.

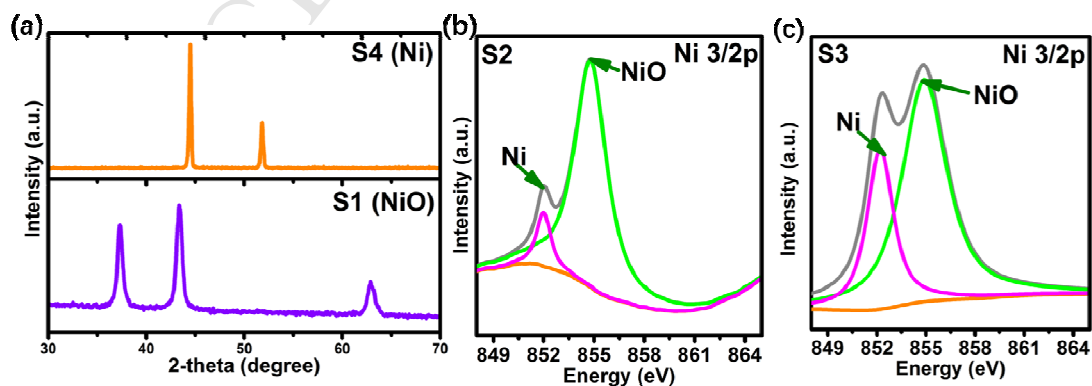


Figure 2.

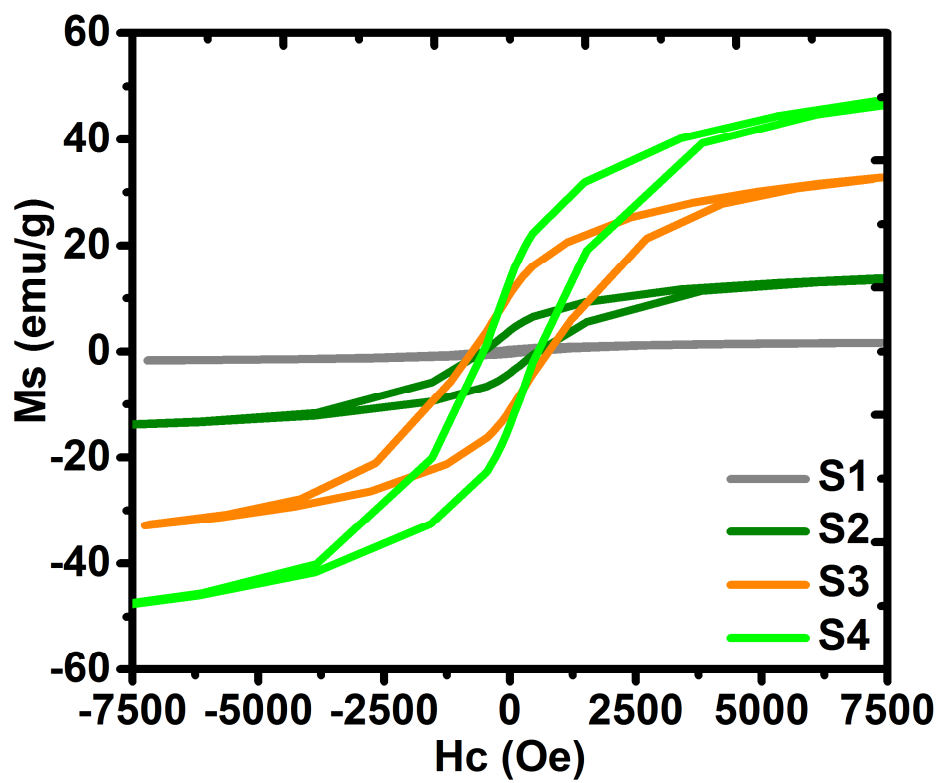


Figure 3.

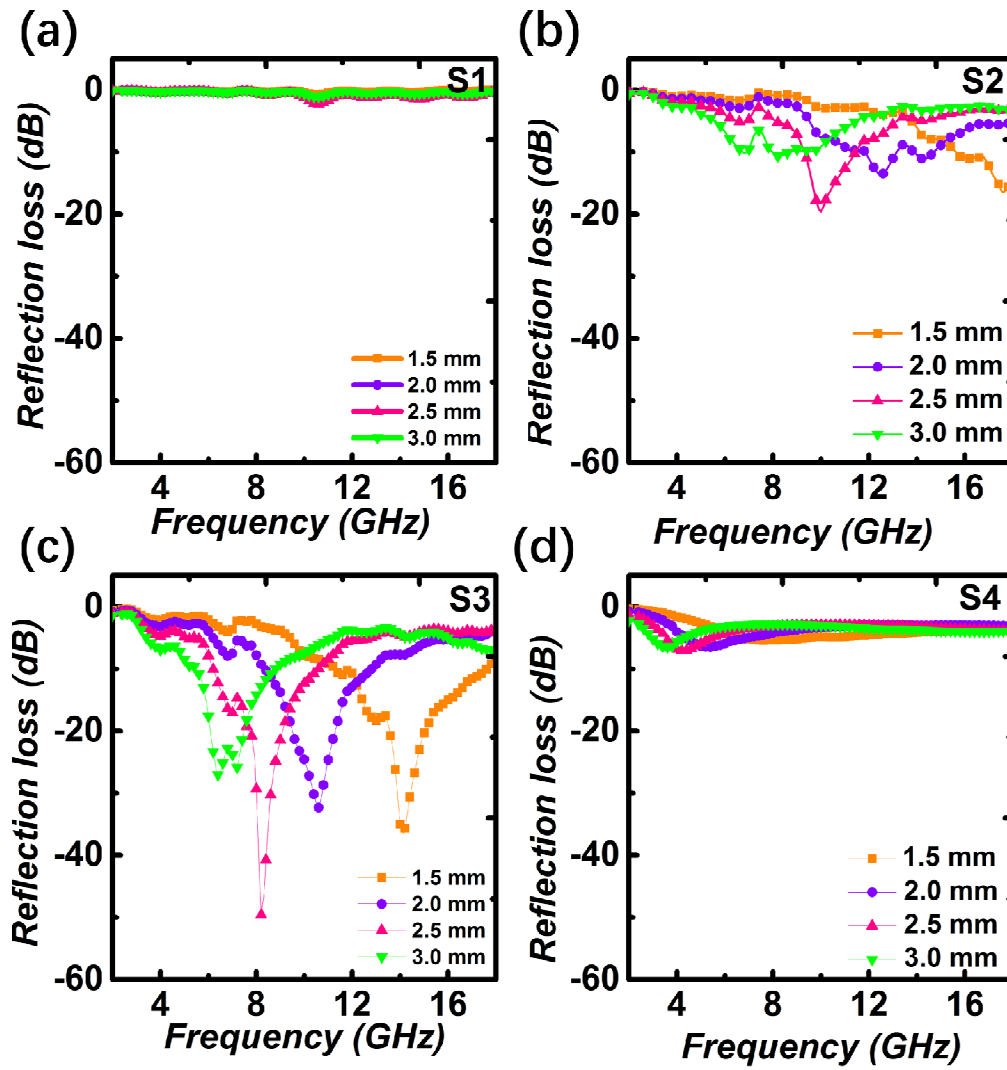


Figure 4.

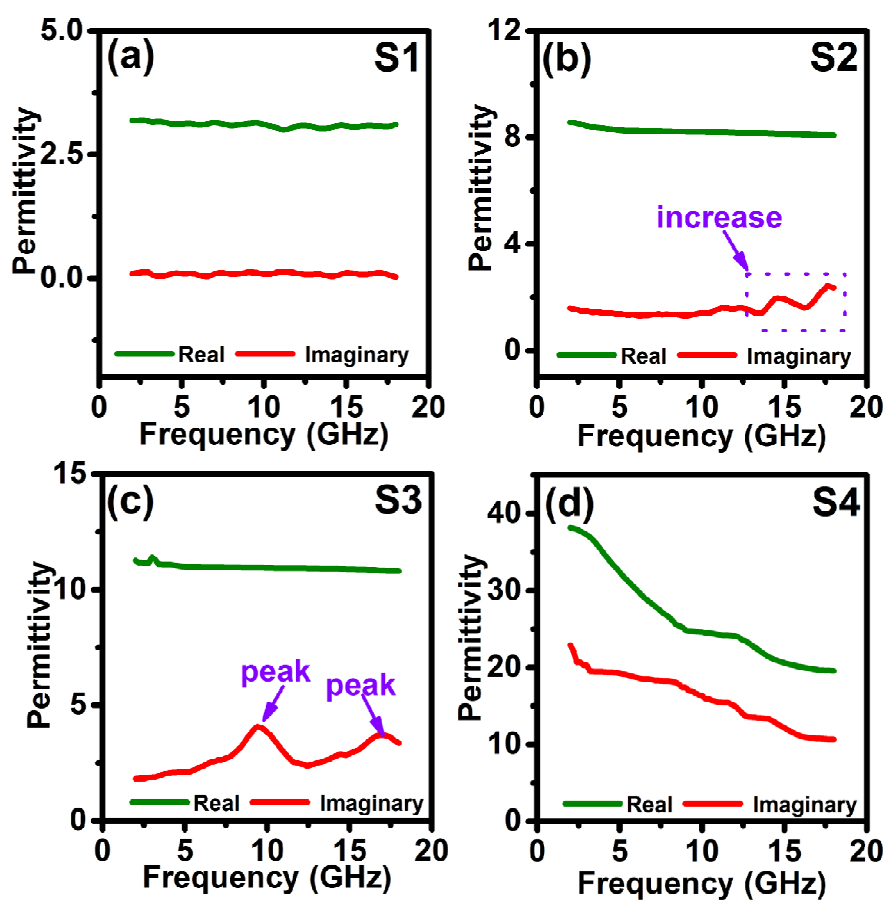


Figure 5.

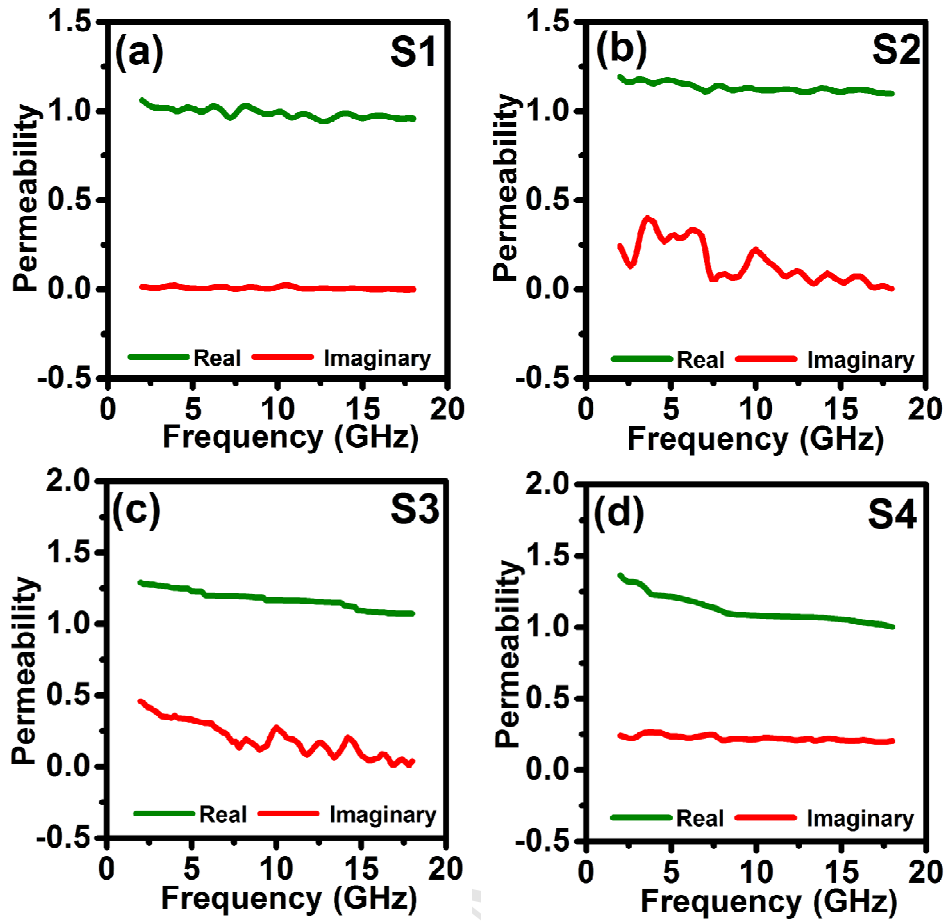


Figure 6.

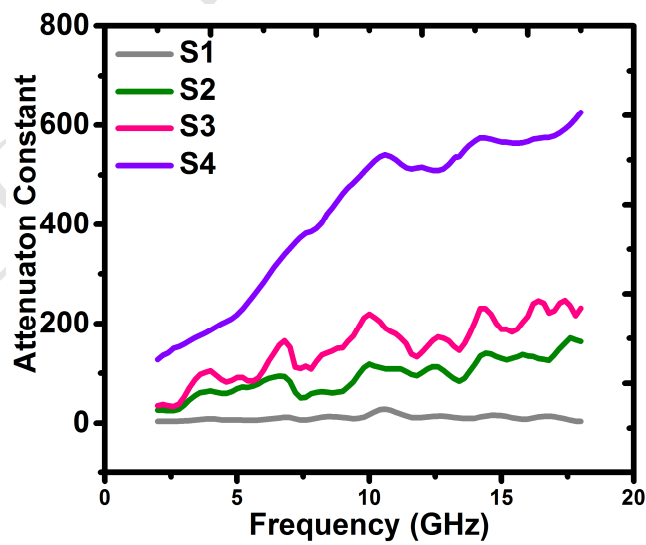


Figure 7.

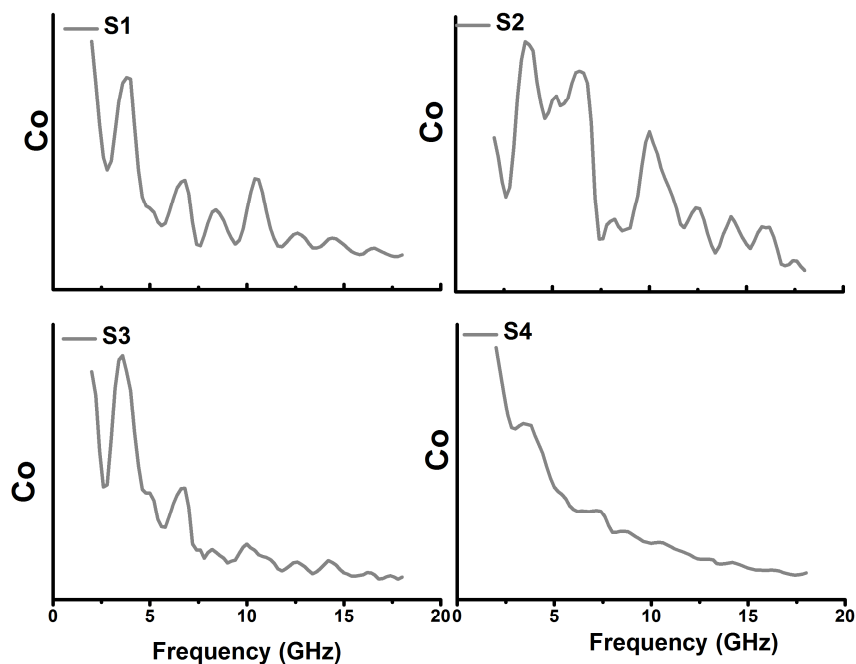


Figure 8.

Captions:

Figure 1: (a): The XRD patterns of the Ni/NiO porous disk-like composite; (b-c): The low-resolution TEM images of the Ni/NiO composites; (d): The High Resolution TEM (HRTEM) image of the Ni/NiO composite;

Figure 2: The XRD patterns of the samples prepared with 0 and 15 mL hydrazine hydrate; (b): The XPS spectrum of Ni/NiO sample obtained with 5 mL hydrazine hydrate; (c): XPS spectrum of Ni/NiO sample obtained with 10 mL hydrazine hydrate;

Figure 3: The magnetization values of the four samples. (S1-S4);

Figure 4: The reflection loss images of the samples prepared with various of hydrazine hydrate; (a) S1 (0 mL); S2(5 mL); (c) S3(10 mL); (d) S4 (15 mL);

Figure 5: The real/imaginary part permittivity values of the samples prepared of the S1-S4 samples: (a) S1; S2; (c) S3; (d) S4;

Figure 6: The real/imaginary part permeability values of the samples prepared of the S1-S4

samples: (a) S1; S2; (c) S3; (d) S4;

Figure 7: The attenuation constant of the S1-S4 samples;

Figure 8: The $Co-f$ curves of the four samples; (a) S1; S2; (c) S3; (d) S4;

ACCEPTED MANUSCRIPT

Highlights:

- 1) The porous disk-like structure is able to suppress the unwanted eddy current effect.
- 2) The partial reduction of NiO benefits to the impedance matching and attenuation electromagnetic ability;
- 3) The electromagnetic absorption performance was tunable by adjusting the reduction degree.
- 4) The optimal qualified absorption frequency bandwidth could up to 6.2 GHz while the thickness was only 1.5 mm.